1   **Spatial and temporal simulation of groundwater recharge and cross-**

2   **validation with point measurements in volcanic aquifers with variable**

3   **topography**

4   Alemu Yenehun[a,b], Mekete Dessie[c], Fenta Nigate[a], Ashebir Sewale Belay[a,b], Mulugeta Azeze[c], Marc Van Camp[b],

5   Derbew Fenetie Taye[f], Desale Kidane[e,f], Enyew Adgo[f], Jan Nyssen[g], Ann van Griensven[d], Kristine Walraevens[b]

6   [a]*School of Earth Sciences, Bahir Dar University, Bahir Dar, Ethiopia*

7   [b]*Laboratory for Applied Geology and Hydrogeology, Department of Geology, Ghent University, Gent, Belgium*

8   [c]*Faculty of Civil and Water Resources Engineering, Bahir Dar University, Bahir Dar, Ethiopia*

9   [d]*Department of Hydrology and Hydraulic Engineering, Vrije Universiteit Brussel, Brussel, Belgium*

10   [e]*Department of Soil Physics, Ghent University, Belgium*

11   [f]*Department of Natural Resources, Bahir Dar University, Ethiopia*

12   [g]*Department of Geography, Ghent University, Belgium*

13   Correspondence to: Alemu Yenehun (abrexyene@email.com)

14   *Abstract*

15   A physically distributed water balance model called WetSpass is applied to estimate the

16   recharge for the semi-humid Lake Tana basin in northwest Ethiopia. Lake Tana basin is one of the

17   growth corridors of the country, where huge waterworks infrastructure is developing. Estimating

18   groundwater recharge at required spatial and temporal scales is a challenge in groundwater

19   management, sustainability and pollution studies. In this study, the WetSpass model is developed

20   at 90 m grid resolution. The spatial recharge map by WetSpass is cross-validated with water table

21   fluctuation (WTF) and chloride mass balance (CMB) methods. The mean annual recharge, surface

22   runoff, and evapotranspiration over the whole basin using WetSpass are estimated at 315 mm, 416

23   mm, and 770 mm of rainfall, respectively. The mean annual recharge ranges from 0 mm to 1085

24   mm (0% to 57% of the rainfall): 0 mm at water bodies and highest on flat, sandy loam soil and

25   bush land cover. Similarly, a high range of recharge is also noted using WTF and CMB methods

26   showing the strong heterogeneous nature of the hydro(meteoro)logical characteristics of the area.

27   Generally, the recharge is found higher in southern and eastern catchments and lower in the

28   northern catchments, primarily due to higher rainfall amounts in the former parts. A fair general

29   correlation between the recharge by WTF and WetSpass is found. WetSpass is effective in aquifers

30   where diffuse recharging mechanism is the predominant type and recharge is controlled by rainfall.

31   It is less effective in the storage-controlled flat floodplain alluvial and fractured rock aquifer areas.

32   In these areas, the point estimates by WTF and CMB are effective and can be considered as reliable

33   values. The land use change from 1986 to 2014 brought a relatively small hydrological change in

34   recharge although the land use has changed significantly.

35   Keywords: **Lake Tana basin; recharge; WetSpass; WTF; CMB; storage controlled; diffuse**

36   **recharge**

1. Introduction

38   Groundwater recharge is all water that reaches the groundwater aquifer from any direction

39   (Scanlon et al., 2002). In specific terms, it is defined as the height of the water column that enters

40   the groundwater zone after crossing the vadose zone in a specific period (Manna et al., 2016).

41   Understanding recharge processes and its quantification is vital for proper management and

42   protection of the limited groundwater resources (Ferede et al., 2020; Healy and Cook, 2002;

43   Uugulu and Wanke, 2020). However, it is one of the most difficult water balance components to

44   be evaluated with acceptable accuracy (Hornero et al., 2016). This is particularly true in areas with

45   wide heterogeneity of geological, topographical, and hydro-climatic conditions. Thus,

46   groundwater water management and development policymakers and practitioners should take

47   recharge estimations and their uncertainty into account in the management plans (Hornero et al.,

48   2016). As recharge processes significantly vary from area to area, there is no guarantee that one

49   method effectively used for one locality will give reasonable results when applied for another

50   (Obuobie et al., 2012). Different methods are developed for recharge estimation. However,

51   choosing appropriate methods is often challenging. Important considerations in choosing a

52   technique include space/time scales, range, and reliability of recharge estimates which in turn

53   depend on the goal of the study (Scanlon et al., 2002). Fore instance, groundwater resources

54   assessment of an area may be achieved at a small space/time scale but flow and contaminant

55   modeling need quantification of recharge amounts at large spatial as well as temporal scales.

56   There is a strong groundwater recharge variability across the Ethiopian volcanic rock aquifers

57   (Alemayehu and Kebede, 2011; Ayenew et al., 2008; Demlie et al., 2008, 2007b; Kebede et al.,

58   2005). Lake Tana basin, which is one of the major basins in the Ethiopian volcanic plateau, has

59   high hydrogeological and topographical variabilities. Furthermore, the area has a climate with long

60 dry winters and short rainy summer seasons. Hence, the groundwater recharge-discharge processes

61 are expected to vary highly both spatially and temporally. There are a number of recharge

62 estimation methods whose effectiveness depend on the recharge mechanism (Healy and Cook,

63 2002). Hence, understanding and identifying the recharging mechanism of aquifers and the

64 assumptions of different estimations methods is a key to effectively choose among the different

65 techniques (Scanlon et al., 2002; Tilahun et al., 2009). On fractured aquifers where preferential

66 flow dominates, focused recharge is a major recharge mechanism rather than the diffuse recharge.

67 Water balance models estimate better the diffuse recharge (Zhu et al., 2020), while water point

68 measuring-based methods such as water table fluctuation are preferable for focused recharge

69 mechanisms (Scanlon et al., 2002). One of the challenges for the point recharge estimation

70 methods is their incapability to estimate it in a spatially distributed way. Given the high spatial

71 variability of recharge, due to variations in geology, topography, soil texture, land use, and

72 meteorological variables, it is unwise to extrapolate or regionalized the result by the conventional

73 point recharge estimation techniques (Tilahun and Merkel, 2009). Hence, in this study, a

74 physically-based water balance model called WetSpass, which simulates recharge in a spatially

75 and temporally distributed manner is applied. Water table fluctuation and chloride mass balance

76 methods have been used to identify the recharge mechanisms, to compare and cross-validate the

77 result by the WetSpass model. These methods have been applied in several studies: the WetSpass

78 model for example in Batelaan and De Smedt (2007, 2001), Gebreyohannes et al. (2013), Graf and

79 Przybyłek (2018), Salem et al. (2019), Ashaolu (2020), Yenehun et al. (2020); the WTF method

80 for example in Sophocleous (1991), Healy and Cook (2002), Moon et al. (2004), Crosbie et al.

81 (2005), Chal et al. (2006), Mikunthan and De Silva (2009), Nigate et al. (2020), Yenehun et al.

82 (2020); and the CMB method for example in Allison and Hughes (1978), Allison (1988), Guan et

83 al. (2010), Somaratne and Smettem (2014), Uugulu and Wanke (2020), Yenehun et al. (2020).

84   The main objectives of this study are: 1) to determine groundwater recharge of the Lake Tana

85 basin in a spatially distributed way; 2) to identify controlling factors for the spatial variability of

86 the recharge in the basin; 3) to compare and evaluate the recharge estimation methods over the

87 basin; 4) to evaluate the effect of land use change over the hydrology of Lake Tana basin, and 5)

88 to determine the spatial and seasonal variation of runoff and evapotranspiration in the basin.

2. Study area location, geology, and hydrogeology

89

90   The Lake Tana Basin (Fig. 1) consists of the Lake Tana water body which is the largest natural

91   lake in Ethiopia. It is the source and head of the upper Blue Nile Basin which is the major tributary

92   to the Nile Basin. The Nile Basin is shared by eleven riparian countries and is the lifeline for more

93   than 238 million people living in the basin (Dile et al., 2018; Tekleab et al., 2011). Lake Tana

94   Basin has a total drainage area of approximately 15,077 km^2, of which the lake covers about 3,077

95   km^2. It is a shallow lake, which is situated in the northwestern Ethiopian highlands and receives

96   flow from more than 40 rivers (Dessie et al., 2015, 2014; Rientjes et al., 2011; Wale et al., 2009).

97
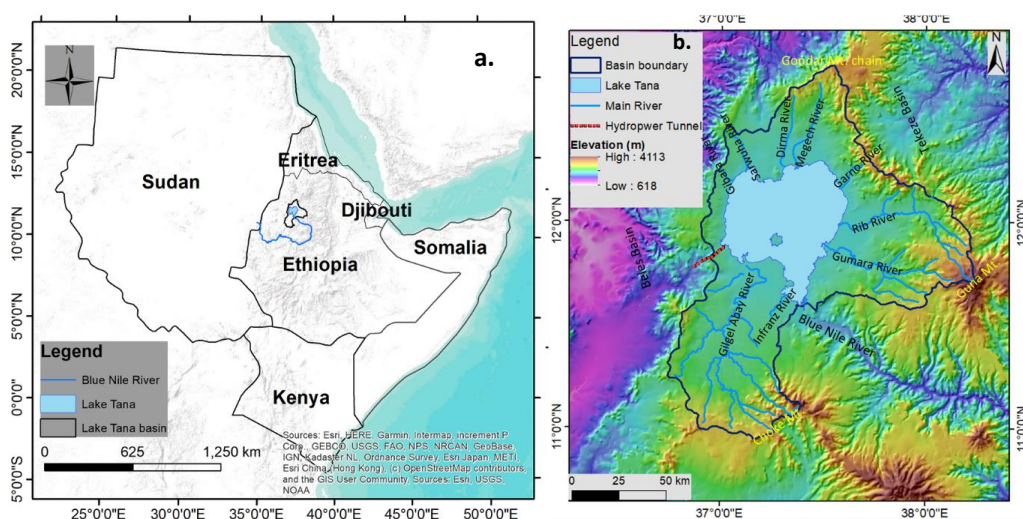
98   *Fig. 1. Location map of Lake Tana basin showing the location of the Lake Tana basin within Ethiopia*

99   *and its neighbors (a), and topographical setup and main rivers (b). The Beles, the Blue Nile, and the*

100   *Tekeze basins are the major adjacent basins for Lake Tana Basin.*

101   The Lake Tana basin is perched on a topographic high which is within an overall configuration

102   of an uplifted dome that was active during the Tertiary volcanic events. The Lake Tana basin was

103   formed by the junction of three grabens (Chorowicz et al., 1998). It acquired its present form

104   through damming by Quaternary lava flow aged to 10,000 years on its southern part (Jepsen and

105   Athearn, 1961). Stratified Tertiary volcanic rock piles in northwestern Ethiopia overlie Mesozoic

106   sedimentary rock stratigraphical sequence (Chorowicz et al., 1998). They have an average

107   thickness of 1 to 1.5 km (Jepsen and Athearn, 1961; Minucci, 1938), and covers a significant area

108   of the basin (Fig. 2). Quaternary basalt covers most of the southern part of the Tana Basin (Jepsen

109 and Athearn, 1961). Sedimentary deposits such as the Pliocene Chilga sediment and recent alluvio-

110 lacustrine sediments on the extensive floodplains of the northern and eastern catchments are also

111 among major lithological coverages (Fig. 2).
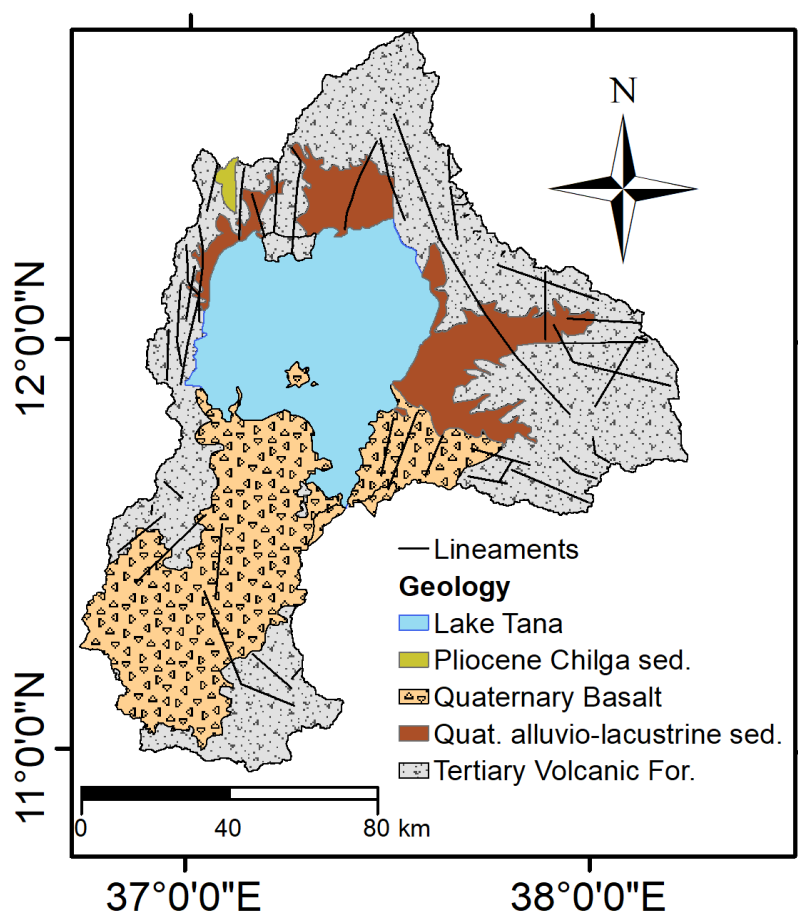
113 *Fig. 2. Geological map of Lake Tana basin modified after* Nigate (2019).

114   The complex nature of the aquifers, owing mainly to multi-stage volcanism at different

115 volcanic centers, and hence the presence of different volcanic rock types (with complex

116 geometrical setting) in the Ethiopian volcanic plateau, has led to a strong spatial groundwater

117 potential and recharge variability (Alemayehu and Kebede, 2011; Ayenew et al., 2008; Demlie et

118 al., 2008, 2007b; Kebede et al., 2005).. The water level for aquifers lying at different physiography

119 in the highlands of the Lake Tana basin responds differently to the rainfall and has a different

120 recharging mechanism (Yenehun et al., 2020).

3. Data and methods

3.1. WetSpass model

For this study, the WetSpass model written in Python (WetSpass-M) is applied. The WetSpass (an acronym for Water and Energy Transfer in Soil, Plants, and Atmosphere under quasi Steady State) was first developed by Batelaan and De Smedt (2001) and later modified by Batelaan and De Smedt (2007). It is a numerical model to simulate long-term average spatial distributions of hydrological parameters and processes at a basin-scale in quasi-steady state. It means the model is restricted to temporal variations only at the seasonal or monthly time scale. That means years of seasonal or monthly time series data are averaged into single seasons or months. The model subdivides the precipitation into the runoff (to refer only to surface component of the river flow in this paper), evapotranspiration, and groundwater recharge, and estimates long-term seasonal values as distributed spatial maps.

$$P = S + ET + R \tag{1}$$

Where P is precipitation [L], S is runoff [L], ET is evapotranspiration [L], and R is groundwater recharge [L].

$$S = f_1 * P_n \tag{2}$$

Where f_1 is a runoff factor that depends on land use and vegetation characteristics, soil texture, and slope. P_n is the net precipitation reaching the ground surface (total precipitation minus interception by the plant canopy).

$$ET = f_2 * EP \tag{3}$$

Where f_2 is an evapotranspiration factor which depends on land use and vegetation characteristics and soil texture, and EP is the potential evaporation of open water [L].

Groundwater recharge is estimated as the closure term of equation 1.

The WetSpass-M model calculates each hydrological term at pixel scale by subdividing each pixel into open water, impervious surface area, bare soil, and vegetated area. Percentage values of these subdivisions of a pixel are assigned for all possible land use classes in the parameter table of the model. However, some percentage values have been modified based on local expert judgment.

148   In this study, the model is developed at 90 m x 90 m grid resolution. Hence, all the nine input

149   parameter grid maps are resampled to the same grid size. The model area is equally meshed and

150   has 1824 columns and 2223 rows. WetSpass has parameter tables as an input besides the grid

151   maps. Some land-use parameter values and the number of rainy days are modified into local

152   contexts based on measured data and our expert knowledge whereas the default values of soil-

153   related parameters have been kept. For example, the root depth for forest land use is changed from

154   2 m to 5.5 m, because eucalyptus (the dominant forest tree in the area) is deep-rooted. A similar

155   modification was made by Yenehun et al. (2020) for the highland part of the Gilgel Abay

156   catchment.

157   The developed WetSpass model is calibrated manually by adjusting the global model

158   parameters, such as rainfall intensity, soil moisture alfa coefficient (α), LPa calibration parameter

159   for adjusting the potential evapotranspiration depending on the soil moisture, interception

160   parameter (a), and runoff delay factor (x). In the calibration process, the goodness of fit between

161   the simulated and measured runoff for major rivers was being checked and has been used for

162   further model optimization. Furthermore, the point recharge values determined by the WTF

163   method and extracted recharge of the WetSpass spatial map are compared, thereby validating the

164   result.

165   For model calibration, the recent land use (land use 2014) (Fig. 4c) has been used. After the

166   model is calibrated to the optimal possible using this land use, the model is run for land uses 1986

167   and 2000 (Figs. 4a and b). Hence, the effect of land use change on the seasonal water balance terms

168   has been evaluated.

3.1.1. Data for WetSpass model

170   Meteorological data consisting of rainfall, temperature (minimum, maximum, average),

171   relative humidity, sunshine hours, and wind speed, and GIS spatial maps including land use, soil

172   texture, elevation, slope angle, and groundwater level have been used for the WetSpass model.

173   The meteorological data were collected from the Ethiopian National Meteorological Agency

174   (NMA), Bahir Dar branch, and our simple meteorological stations (measuring only rainfall and

175   temperature). The WetSpass model uses the long-term average raster grid maps of rainfall,

176   potential evapotranspiration (PET), mean temperature, and wind speed (Batelaan and De Smedt,

177   2007, 2001). The WetSpass model calculates the water balance of an area at a relatively coarse

178 time scale (per month to the finest). However, for semi-humid tropical regions where most of the

179 months are dry winter, applying the model at the seasonal time scale is preferable. Hence,

180 preparation of these data for summer and winter is done. The wet summer consists of months from

181 June to September and the dry winter from October to May. Gebreyohannes et al. (2013) worked

182 similarly for their application of the method at the Geba catchment in northern Ethiopia.

183   The long-term seasonal average point rainfall depth (mostly from 2005 to 2018) is prepared

184 from 50 meteorological stations distributed mainly from the basin and a few from the surroundings

185 (Fig. 3a). 42 of the stations were from NMA, and the remaining 8 were our own. The data from

186 our stations were short-term ones, comprising only 2017 to 2019. The areal rainfall depth maps

187 for both summer and winter are produced through the kriging interpolation since the number of

188 input stations was relatively high and appropriate for this interpolation technique. Mean annual

189 temperature raster maps for both the summer and winter seasons are prepared from 30 stations

190 using the inverse distance weighting (IDW) method. Similarly, IDW is applied for windspeed

191 using data from only 7 socalled first-class meteorological stations (Fig. 3a).

192   For the potential evapotranspiration, the Penman-Monteith method, modified by Allen et

193 al. (1998), is applied to calculate point PET values at 8 stations (Fig. 3a). For the spatial

194 interpolation, IDW is applied and maps for both summer and winter are produced.The mean annual

195 PET map is presented in Fig. 3c. The groundwater depth grid map is needed in the WetSpass model

196 primarily to calculate evapotranspiration from the groundwater, and for delineation of wetlands,

197 so that water balance calculations include seepage fluxes (Batelaan and De Smedt, 2007;

198 Gebreyohannes et al., 2013). Hence, the groundwater level grid maps for both summer and winter

199 seasons are prepared using time series groundwater level data collected for this study. First, an

200 average depth to water table raster map by classifying the area into high middle and low elevations

201 is prepared using our groundwater monitoring points. Then this raster map consisting of three

202 different depth to water table raster values is subtracted from the DEM of the area to obtain the

203 hydraulic head raster ASCII map which is the input of the WetSpass model. A similar method is

204 followed for both summer and winter. Furthermore, the WetSpass model is calibrated using river

205 flow data measured at different major rivers of the basin. Hence, mean annual river discharge data

206 measured by Dessie et al. (2015) in the years 2012-2013 have been taken.

207
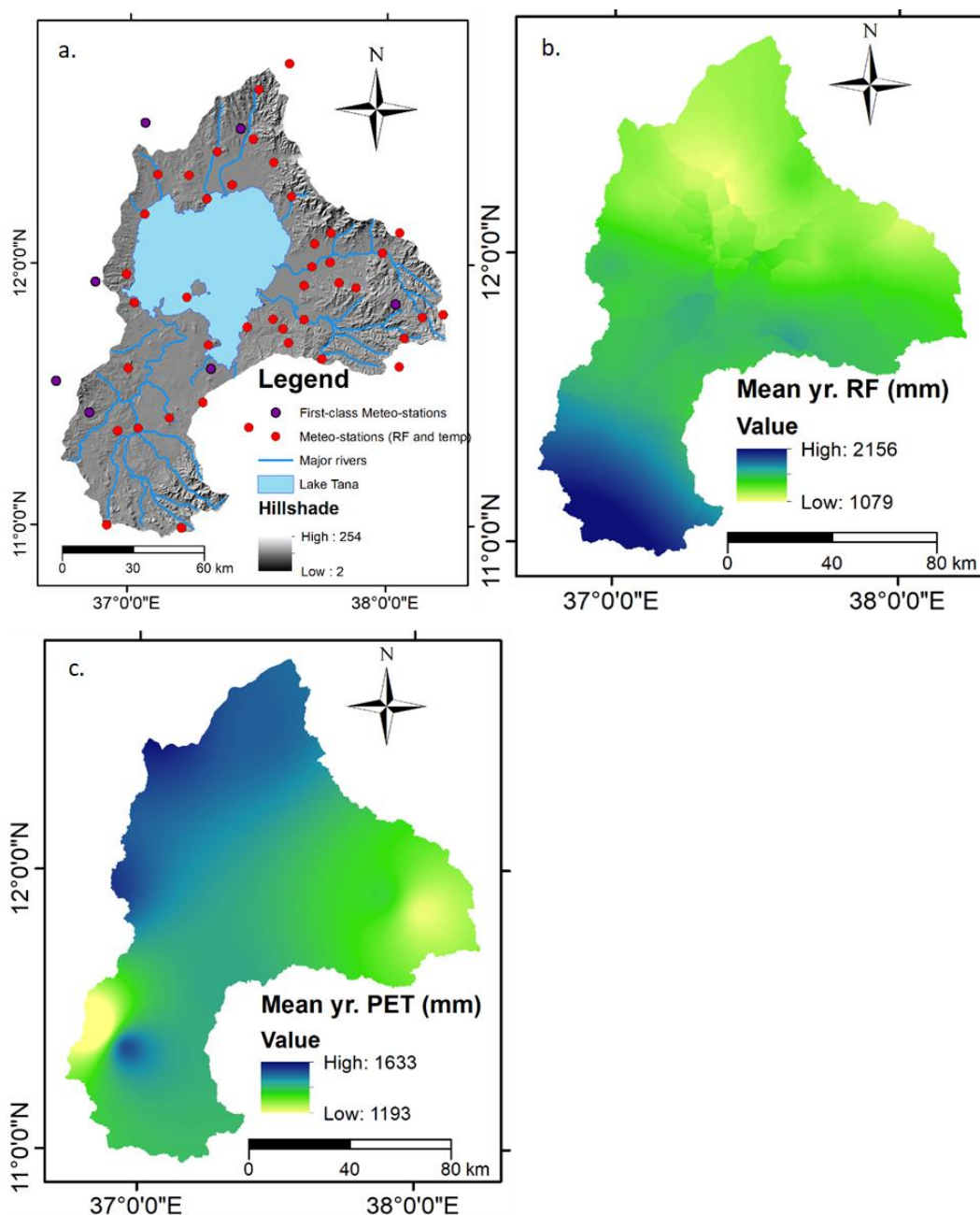
Fig. 3. (a) There are a total of 50 meteorological stations among which eight stations are measuring

minimum and maximum temperatures, rainfall, windspeed, relative humidity, and sunshine hours. (b) The

mean annual rainfall map is produced by Kriging interpolation using data from the 50 meteorological

211   *stations. (c) The long-term mean annual PET map is produced through IDW interpolation from the eight*

212   *first-class meteorological stations. The point PET data were calculated by the Penman-Monteith method.*

213   The rainfall has high spatial variation, with minimum and maximum mean annual of 1079

214   mm and 2156 mm, respectively (with a standard deviation of 216). The rainfall is generally higher

215   in the southern, and lower in the northern parts of the study basin (Fig.3b). The lowers is recorded

216   in the flat floodplain of the northern (Megech) catchment, and highest at the southern highlands

217   (Figs. 1 and 3a, 3b). There is a poor correlation between rainfall and topographical elevation,

218   similar to what was reported by Dessie et al. (2014). The maximum and minimum potential

219   evapotranspiration are 1633 mm and 1193 mm, respectively, and with a mean of 1478 mm and a

220   standard deviation of 70. The higher values on the northwestern, and lower towards the south and

221   eastern highlands (Fig. 3c). There is no generally a good correlation between elevation and PET

222   values. The relatively few numbers of meteorological stations for PET interpolation is one of the

223   limiting factors in this study.

224   GIS spatial maps are taken from different sources and adapted according to the model

225   requirement of the WetSpass model. The historical land use maps were prepared by the Amhara

226   Design and Supervision Water Works Enterprise (ADSWE) (ADSWE, 2015a). They had prepared

227   land use maps for the years 1986, 2000, and 2014 using satellite images (SPOT and Landsat) and

228   Google Earth, as well as ground-truthing. Each land use type coverage and change of the

229   classification periods are presented (Table 4). The coding number assigned for land use types in

230   the WetSpass model is given for each class so that the model can read and related with land use

231   parameter table. Appropriate correspondence between the local land use classes and the model

232   parameter tables has been made.
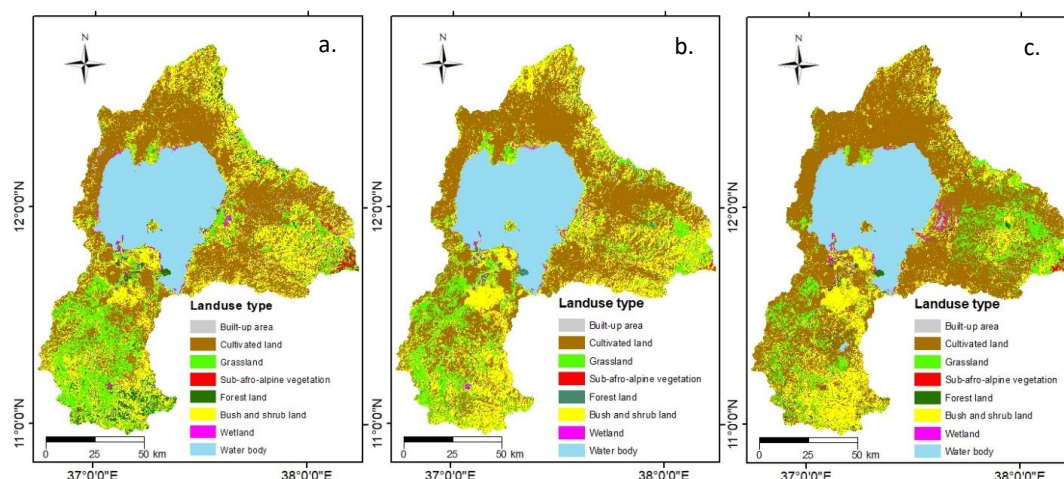
Fig. 4. Land use map of 1986 (a), 2000 (b), and 2014 (c) prepared by the Amhara Design and Supervision Water Works Enterprise.

Table 1. Classified land use types areal coverage in km^2 and percentage of each cover type to the total area of the Lake Tana basin at different years.

Cover type	Area coverage (in km^2) in the classification years and % of each class					
	1986	%	2000	%	2014	%
Built-up area	148.7	1	42.8	0.3	43.6	0.3
Cultivated land	5,530.2	36.7	6,151.9	40.8	7,383.6	49
Grass land	1,822.2	12.1	1,575.9	10.5	1,434.6	9.5
Sub-afro-alpine vegetation	122	0.8	10.6	0.1	38.2	0.3
Forest land	656.8	4.4	349.2	2.3	271.6	1.8
Bush and shrub land	3,640	24.1	3,784.7	25.1	2,688.1	17.8
Wetland	107.1	0.7	100.2	0.7	118.2	0.8
Water body	3,051.2	20.2	3,062.9	20.3	3,100.4	20.6
Total	15,078	100	15,078	100	15,078.2	100

The soil map of the Tana basin used for the modeling is prepared by ADSWE (ADSWE, 2015b). It was prepared through a detailed field survey, sampling, and analysis aided by satellite

240   image information. The soils of the basin were identified and classified based on soil genesis,

241   morphological and surface characteristics according to FAO (1998, 2006) soil map of the world.

242   The results of this soil resource assessment reveal that twelve major agricultural soil types are

243   present in the study area. However, WetSpass needs textural soil classes. Textural classes have

244   been given for most of the 101 mapping units. But for a few of the mapping pixels, the textural

245   class column was found blank in the attribute table of the soil map, and thus we have filled it based

246   on the association of major soil type and common texture in the other mapping units. We have also

247   used our expertise area knowledge in filling these gaps. Finally, codes for each of the seven textural

248   soil classes (Fig. 5a) are assigned, as per in the WetSpass model.

249   A digital elevation model (DEM) with 20 m resolution is found from the Global Land

250   Cover Facility (http://gdem.ersdac.jspacesystems.or.jp/). After filling the possible holes,

251   resampling to 90 m was done and the final raster map for elevation has been prepared (Fig. 5b).

252   Similarly, the slope angle is extracted in ArcGIS 10.3 from the DEM and resampled to 90 m

253   resolution (Fig. 5c).

254
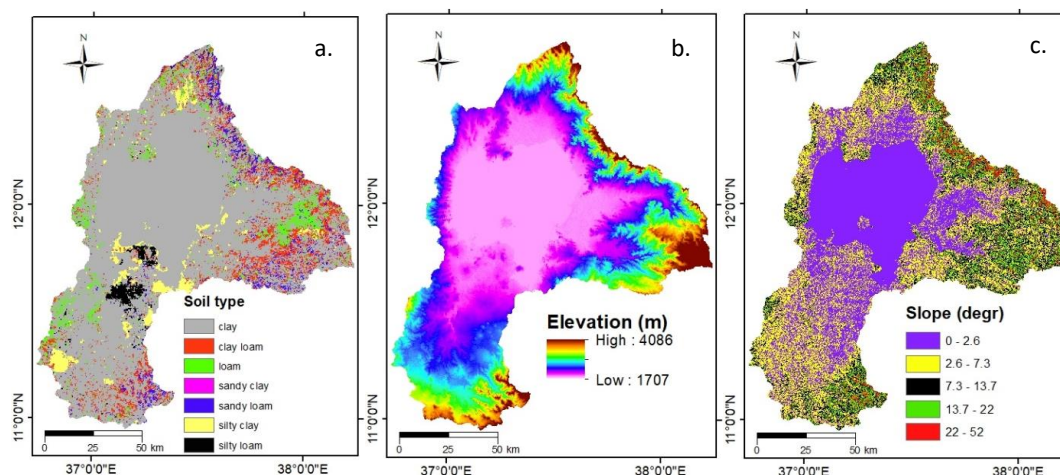
255   *Fig. 5. The soil (a), the elevation (b), and the slope angle (c) spatial maps of the Lake Tana basin*

256   *with a resolution of 90 m*

3.2. Water table fluctuation (WTF) and Chloride mass balance (CMB) methods

The WTF method is among the most widely used techniques for groundwater estimation of aquifers (Healy and Cook, 2002). The method has been applied in many studies (e.g., Sophocleous, 1991; Healy and Cook, 2002; Moon et al., 2004; Crosbie et al., 2005; Chal et al., 2006; Mikunthan and De Silva, 2009, Yenehun et al., 2020). The method uses the following formula to calculate recharge:

$$Recharge = Sy\frac{\Delta h}{\Delta t} \tag{4}$$

where Δh is the head change comparing before and after the rainfall season, Sy is the specific yield, and Δt is the time interval for the recharge period.

According to Delin et al. (2007) and Healy and Cook (2002), for the application of the WTF method, the following assumptions should be satisfied: 1) sharp water level rises and declines in response to only groundwater recharge and discharge; 2) the aquifer system needs to be unconfined with shallow water level; 3) the specific yield should be known and constant. Hence, the monitoring well hydrographs are evaluated, and only those which are more or less in line with these assumptions are considered for the point recharge calculation of this study. Similar to the suggestion of Healy and Cook (2002), the graphical method is applied to extrapolate the recession of the pre-recharge water level to the recharge period so that the water level fluctuation is accurately considered. The main source of uncertainty for the application of the method is the possible errors in the estimation of the specific yield (Healy and Cook, 2002; Yenehun et al., 2020). In this study, both literature from Johnson (1967), and an empirical formula developed by Beretta and Stevenazzi (2018) have been applied. Beretta and Stevenazzi (2018) developed a relationship between Sy and hydraulic conductivity (k). Hence, using the formula, Sy values for monitoring wells were determined using the k values analyzed from our single well pumping and slug test results.

Similar to WTF, the chloride mass balance (CMB) method is a widely applied technique for estimating recharge (Somaratne and Smettem, 2014). The main concept in the method is that the increase in the concentration of chloride in the groundwater compared to the rainwater is due to evapotranspiration in the vadose zone during infiltrating/percolating (Allison and Hughes, 1978;

286   Allison, 1988; Guan et al., 2010; Somaratne and Smettem, 2014). It means chloride anion is a

287   conservative ion and its concentration increment during its movement in the vadose zone is merely

288   in response to evapotranspiration. Mathematically, groundwater recharge (GWR) is calculated in

289   the following way:

290   $GWR = Pe * \frac{Cl_p}{Cl_{gw}}$ (5)

291   Where GWR is groundwater recharge, Cl_p is chloride concentration in precipitation, Cl_{gw} is

292   chloride concentration in groundwater, Pe is effective precipitation, which is the total precipitation

293   minus runoff amount of the period.

294   In this study, the recharge calculation using the CMB has been made by subdividing the

295   basin into southern, eastern, northern, and western catchments. Hence, the average chloride

296   concentration in the analyzed groundwater and rainfall sampled in the specific sub-area is

297   considered. These subdivisions are based on similar runoff characteristics and runoff coefficients

298   in the four distinguished catchments (Dessie et al., 2015). The mean annual rainfall within the

299   respective areas, and mean annual runoff estimated by Dessie et al. (2015) separately for the four

300   sub-areas are considered for the effective precipitation calculation.

301   ### 3.2.1. Data for WTF and CMB methods

302   In this study, the water table fluctuation and the chloride mass balance methods are also used

303   to estimate recharge besides the WetSpass water balance model, to independently verify and

304   compare the spatial estimation. Hence, high-frequency water level data logging and water

305   sampling for chloride and associated chemicals have been executed.

306   Water level data were being collected from May 2017 to June 2019 using 65 shallow hand-

307   dug and piezometer wells using community-based manual daily measurement and automatic

308   measuring sensors at every half an hour interval. We trained the local people, mostly the well

309   owners, and sometimes their neighbors in cases where the owners are illiterate. Afterward, we

310   supplied them with a measuring meter and a rope tied with a steel rod having a length of about

311   half a meter. Every morning before fetching water, they insert this rope tied with the steel rod into

312   the well until it reaches some depth below the water level, and then immediately get it out and

313   measure the depth from the head of the well to the tip of the moist surface on the metal plate. 52

314   of the monitoring wells were large diameter hand-dug wells and had been measured manually

315   using such simple equipment, whereas the other 13 wells were being monitored using automatic

316   data loggers. These 13 wells were both shallow piezometers and deep wells (9 shallow piezometers

317   and 4 shallow borehole wells). The measuring time interval for the manual readings was daily, and

318   for the automatic logging, it was every half an hour. Some of the hand-dug wells are active water

319   supplying wells where the owners fetch water for domestic and/or backyard irrigation purposes.

320   Hence, we order our data recorders to measure the static water level in the early morning when it

321   is preceded by long non-fetching hours (when full recovery is maintained). These monitoring wells

322   are well distributed over the studied basin and representing the various geological and

323   topographical settings.
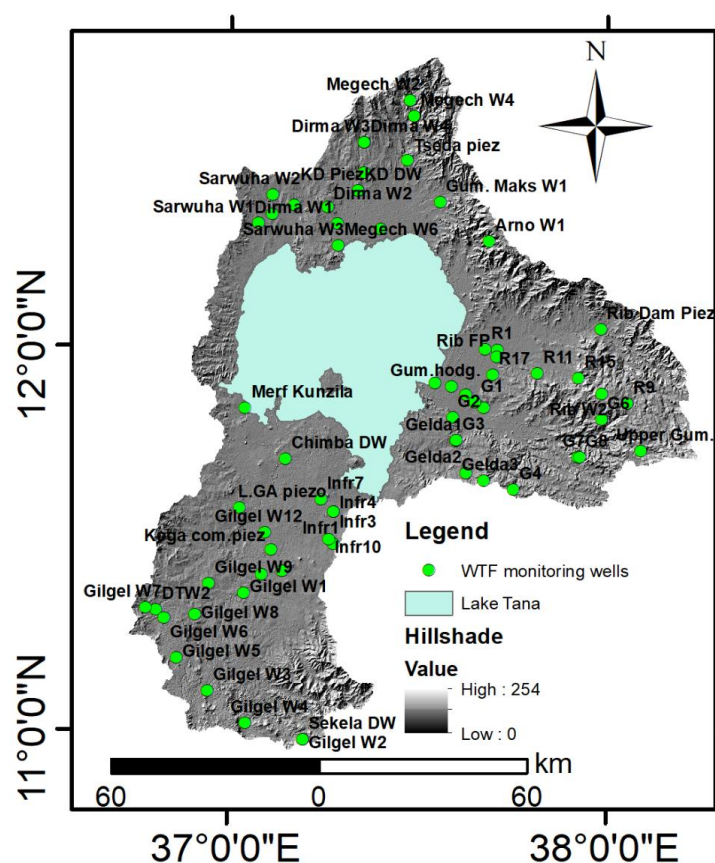
324

325   *Fig. 6. location of 65 monitoring wells used for WTF estimation. Monitored both manually and*

326   *automatically by data logger sensor. Fairly distributed depending on topography and geology.*

327   Water sampling for chemical analysis of the groundwater had been undertaken from 2016 to
328   2019. The sampling sites were distributed throughout the study area representing the different
329   aquifer settings, considering geology and topography. Similarly, rainfall samples had been
330   collected in similar periods at the lower, middle, and upper topography of the basin so that possible
331   topographical influences on the rainfall water chemistry are taken into consideration. In total, about
332   255 groundwater samples and 25 rainfall samples have been collected and analyzed at Ghent
333   University, Department of Geology, Laboratory of Applied Geology and Hydrogeology. Good
334   handling practices of the samples during sampling, storage, and analysis were considered so that
335   evaporation which would increase the concentration of chloride through artificial means is absent.

4.   Result and discussion

4.2.   Spatial and temporal variation of groundwater recharge and other water balance components

339   The calibrated WetSpass model developed using the present land use (2014 land use) presents
340   different water balance components. Among them, the annual groundwater recharge, runoff, and
341   evapotranspiration as spatially distributed digital maps are the primary ones. The annual
342   groundwater recharge ranges from 0 mm to 1085 mm (Fig. 7a) and has a mean value of 315 mm
343   (22% of rainfall amount). Recharge is assumed 0 mm at water bodies and wetlands in the WetSpass
344   model. Hence, recharge is 0 mm at Lake Tana and a dam reservoir in the Gilgel Abay catchment
345   and wetlands in the lower reaches of Rib river catchment (Fig. 4c). No recharge at water body is
346   the general assumption of the WetSpass model. Fortunately, this assumption is in line with
347   previous studies (e.g. Kebede et al., 2006; Mamo, 2015; SMEC, 2008), which had concluded
348   thatthere is insignificant percolation beneath the lake floor. Higher recharge is estimated on the
349   southern (Gilgel Abay) and eastern (Gumara) river catchments (Figs. 1b and 7a), and lower on the
350   northern part of the Lake Tana basin. This is mainly due to the lower rainfall amount in the northern
351   catchments compared to southern catchments (Figs. 3b and 7a). Next to the rainfall, the spatial
352   distribution of the recharge seems highly controlled by the slope angle, followed by the soil type,
353   and the land use type. Forest land covering only 1.8% has high recharge (mean annual of 542 mm).
354   Cultivated land and water body consisting of about 49% and 21% of the total areal coverage, have
355   annual mean recharge values of 370 mm and 0 mm, respectively, dominating over the total average
356   value. Clay soil type, covering about 77% of the total basin area, has a mean annual value of about

357   276 mm, the lowest amount estimated compared to all other soil types. The major recharge is

358   taking place during the summer season while only a small amount recharges during the winter:

359   about 237 mm is recharged in the summer and 78 mm in the winter seasons. The mean annual

360   recharge is about 22% of the total mean basinprecipitation.

361   The mean annual runoff for the whole basin is about 416 mm, accounting for about 29% of the

362   average precipitation. About 92% of the runoff is taking place during the summer season, while

363   the remaining is taking place during the long winter season. Relatively higher runoff is observed

364   in the southern and eastern basins, and lower runoff has been noted in the northern and northeastern

365   (Rib) river catchments (Fig. 7c). This is in line with the study by Dessie et al. (2015). In some

366   areas (e.g. in northern and northeastern), low runoff value has been observed on the cultivated land

367   and clay soil types where a high runoff coefficient is expected (Figs. 4c, 5a, and 7c). This is due

368   to the relatively low rainfall amount on these parts of the Lake Tana basin (Fig. 3b). This shows

369   that compared to the rainfall, the soil type and the land use have less influence over the runoff. The

370   rainfall amount is highly controlling the spatial distribution of runoff (Figs. 3b and 7c). The zonal

371   statistics for the land use and soil classes types show a high variation of runoff over the single class

372   types. For example, for clay soil with cultivated land cover type, the runoff ranges from 212 mm

373   to 1216 mm (15%-84% of mean rainfall), and with an average of 485 mm accounting for about

374   34% of the rainfall. This variation is found mainly due to the variation in the rainfall amount,

375   which is varying from 1097 mm to 2155 mm for the aftermentioned soil and land use class

376   combination. However, it does not mean that the other runoff controlling variables such as the

377   slope are not playing a significant role for such variations.
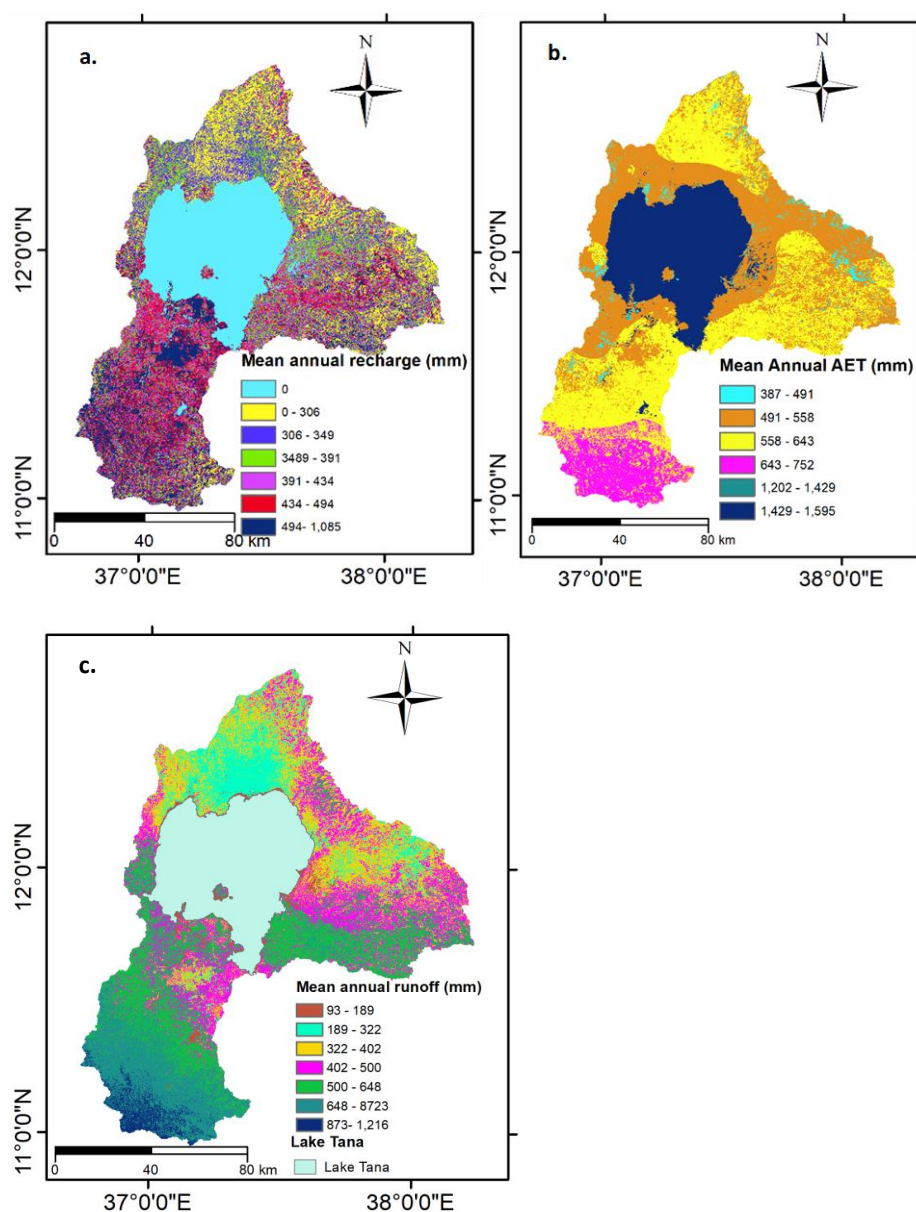
Fig. 7. Long-term mean annual groundwater recharge(a), mean annual actual evapotranspiration (b),
and mean annual runoff (c) spatial maps produced from the WetSpass water balance model.

The evapotranspiration of the Lake Tana basin is mainly the sum of the lake and wetland
direct evaporation and evapotranspiration over the other land cover types. The mean evaporation
over the lake is about 1485 mm. In the WetSpass model, the Penman method is used to estimate

384   the open water evaporation (Batelaan et al., 2007). The average total evapotranspiration over the

385   basin is 770 mm, which is 53% of the mean basin precipitation. About 56% of total

386   evapotranspiration is happening during summer and the other 44% occurs during winter. The mean

387   evapotranspiration of the basin is about 52% of the mean potential evapotranspiration. The spatial

388   distribution of the evapotranspiration over the basin is highly controlled by the rainfall and the

389   land cover types relative to the other physical and meteorological variables (Figs. 3b, 4c, and 7b).

390   It is higher over the lake and wetlands because it is open water where there is no limitation of water

391   availability, and evaporation is equal to the potential evaporation capability of the air. The variation

392   over the lake (Fig. 7b) is due to the variation of the potential evaporation (Figs. 3b and c). Next to

393   the water body and wetlands, grassland, forest, bush and shrubland cover types have high

394   evapotranspiration values.

395   The direct lake water evaporation is compared with other studies estimated by different

396   methods (Table 2). The result is very close to that of Kebede et al. (2006) and Chebud and Melesse

397   (2009) which both used the similar Penman method, and similar time scale (Table 2). However, it

398   is lower than the value estimated by Dessie et al. (2015) which used recent data from six stations.

399   This could be due to the application of different period data (from 2012-2013 while it is from

400   2005-2018 in this study) or the time scale applied (seasonal versus daily) for the calculation or it

401   might be due to the method they used (Table 2). Time scale affects evapotranspiration calculations,

402   which are higher for fine time scales (e.g. daily), and relatively lower for coarser time scales (e.g.

403   seasonal or monthly) (Bakundukize et al., 2011; Yenehun et al., 2020).

404   *Table 2. Simulated mean annual evaporation over the lake of the WetSpass water balance model, and other studies.*

405   *The time scale for the modeling, the period that the meteorological data used and the number of meteorological*

406   *stations, and the estimation technique are indicated.*

Literature	Timescale	Data period used	Number of stations	Estimation method applied	Annual over-lake evaporation (mm)
This study	seasonal	2005-2018	7	Penman (WetSpass)	1458
Wale et al. (2009)	daily	1992–2003	2	Penman-combination equation	1690

Rientjes et al. (2011)	daily	1994–2003	1	Penman-combination equation	1563
Kebede et al. (2006)	daily	1960–1992	1	Penman	1478
SMEC (2008)	monthly	1960–2005	2	Penman	1697
	monthly	1960–1995		Energy balance	1657
Mamo (2015)	monthly	1995–2009	1	Penman	1544
Setegn et al. (2008)	daily	1978–2004	not explicitly mentioned (probably 2)	Hargreaves	1248
Dessie et al. (2015)	daily	2012–2013	6	Penman-combination	1789
Chebud and Melesse (2009)	monthly	not mentioned	1	Penman	1458

4.2.1. Model verification

The developed model is verified using two ways. First, the annual total river discharge observed by Dessie et al. (2015), using the daily time scale data of river discharge of 2012-2013 at seven major rivers, is compared with the corresponding WetSpass model results. These data have been used for the calibration of the model. The river discharge measured by Dessie et al. (2015) for these major perennial rivers is the total flow amount (comprising both surface and baseflow). However, the WetSpass model calculates the runoff (only the surface runoff) but not the total discharge. Hence, to estimate the total river flow at the catchment outlets of each river, we applied a similar technique that Gebreyohannes et al. (2013) had followed. Based on groundwater balance in the aquifers, the long-term average annual groundwater drainage and possible abstractions are equal to the long-term average annual recharge. Given the river gauging stations are usually at the groundwater discharge zones (on the floodplain), the flow measurements are assumed to catch the baseflow component except for a very small amount that may pass through deep percolations. Besides, the groundwater abstractions using different shallow and deep wells can be assumed small compared to natural drainage and recharge as there is no large development of the groundwater in the basin. Using ArcGIS 10.3 tools, both annual runoff and groundwater recharge outputs of the WetSpass model, are accumulated at the river outlets. Finally, the accumulated raster maps of runoff and recharge for each major catchment are summed up to produce the spatial total river discharge map. The total river discharges estimated in this study and those observed by Dessie et al. (2015) are compared (Fig. 8). The overall coefficient of determination (R^2) between the simulated and the observed river discharge values of the different

428   rivers is about 80%. However, for Rib, Dirma, Gelda and Megech river catchments, the simulation

429   by WetSpass is higher compared to the observation by Dessie et al. (2015) (Fig. 8). This could be

430   due to significant deep percolation of the groundwater that is not caught by the river flow

431   measurements i.e. the baseflow is far less than the groundwater recharge.. The model is best

432   simulated for Gilgel Abay and Gumara rivers (Fig. 8). This could be due to the catching up of the

433   baseflow in the flow measurements as most of the groundwater discharges through different

434   springs in the lower reach of the rivers. Similarly, SMEC (2008), and later Dessie et al. (2015,

435   2014) came up with the conclusion that there is significant groundwater contribution for Gilgel

436   Abay and Gumara rivers flow while only little for Megech and Rib. Furthermore, Setegn et al.

437   (2008) had estimated the groundwater (as baseflow) contribution of the whole basin to be 50% of

438   the total river inflow to the lake. It should be noted that the WetSpass model applied is quasi-

439   steady state, and uses long-term average seasonal rainfall, whereas, in reality, the rainfall

440   characteristics (intensity, frequency and duration) vary within fine time scales. This is limiting the

441   effectiveness of the model in simulating runoff.
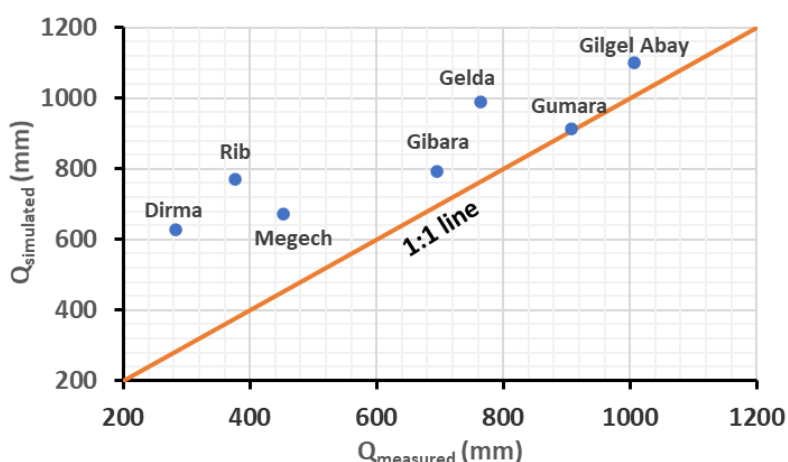
442

443   *Fig. 8. A 1: 1 line between measured mean annual river flow obtained from Dessie et al. (2015) and*

444   *simulated mean annual river flow by WetSpass water balance model for the major rivers in the Lake Tana*

445   *basin. The simulated river flow is calculated by summing up the runoff and the groundwater recharge*

446   *values of each catchment by assuming all the recharge in the upper catchments emerges as an outflow in*

447   *the lower floodplain parts.*

448   The second way that the developed WetSpass model verification made is through its

449   performance in estimating groundwater recharge. The point recharge estimated using the WTF

450   method has been used to compare the model performance at those points. The extracted recharge

451   values of the model were correlated against the WTF results calculated at 65 monitoring stations

452   (Fig. 9a). The overall correlation was fair (with a coefficient of determination, $R^2 = $ 35%).

453   However, Yenehun et al. (2020) evaluated the performance of the WetSpass model in estimating

454   recharge at a small catchment in the upper Gilgel Abay river catchment and found that the

455   technique is less effective at storage controlled flat floodplain areas and at aquifers where focused

456   recharge (through rock fractures) is an important recharging mechanism. Therefore, we excluded

457   WTF results estimated at aquifers on those topographies, and then the correlation coefficient (R^2)

458   is found to be 84% (Fig. 9c). When only two wells located at storage controlled floodplain aquifer

459   named DTW2 and at exceptionally highly fractured aquifer called Sarwuha W1 (Fig. 6) are

460   excluded, the R^2 raised to 71% (Fig. 9b). Hence, the WetSpass method is found effective in

461   estimating the groundwater recharge in most parts of the study basin. However, at the flat

462   floodplain alluvial aquifer and fractured rock aquifers where the hard rock is exposed to the

463   surface, water balance techniques such as the WetSpass are found less effective.
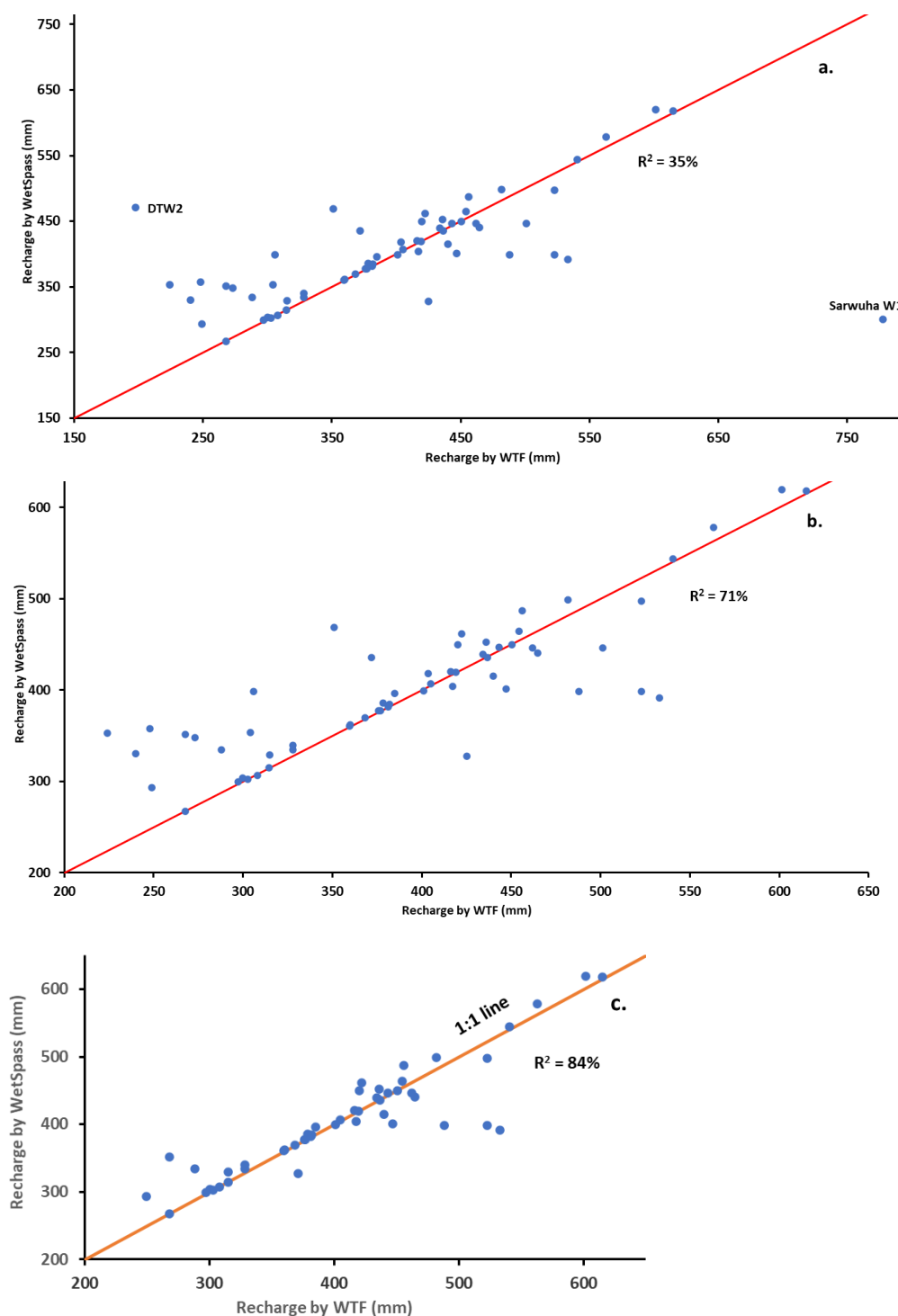
465   *Fig. 9. a) Mean annual recharge by WTF and WetSpass methods at all groundwater monitoring wells.*

466   *The recharge values estimated using WetSpass are extracted at 65 water level monitoring points. It has a*

467   *total correlation of 35%. b) A 1:1 plot of mean annual recharge by WTF versus extracted recharge by*

468   *WetSpass method for monitoring points excluding Sarwuha W1 and DTW2 those strongly affected by*

469   *focused recharge and limited with aquifer storage, respectively. c) A 1:1 plot of mean annual recharge by*

470   *WTF versus extracted recharge by WetSpass method for monitoring points excluding those affected by*

471   *focused recharge and those which are storage controlled on the flat floodplain areas. It has a correlation*

472   *coefficient of 84%.*

4.3. Effect of land use change on groundwater recharge and other water balance components

475   The effect of land use change on groundwater recharge, runoff, and evapotranspiration has

476   been assessed in this study. This assessment has been made using similar long-term average

477   meteorological data, and hence possible variation due to temporal increasing or decreasing of the

478   meteorological variables have not been taken into consideration.

479   The value of water balance terms changes with land use changes. There is a decrease in

480   recharge by 13 mm or $195.9*10^6$ m^3 in the years 1986-2014 (Table 3) in the Lake Tana basin. This

481   is about 4% of the mean annual recharge estimated with the applied WetSpass model. This is inline

482   with the increase of cultivated land area (from 36.7% to 49%), mainly from grass, bush and shrub,

483   and forest lands. Similarly, there is an increase of runoff but it is only by 4 mm or $60.3*10^6$ m^3 in

484   the 28 years (about 1% of the total mean runoff). Similarly, the evapotranspiration shows an

485   increment by 9 mm or $135.6*10^6$ m^3 in these 28 years (about 1.2% of the total mean annual AET).

486   The trend is in line with the studies by Abate et al. (2017), Enku et al. (2014), Gebremicael et al.

487   (2013), Hurni et al. (2005), Tesemma et al. (2010), and Woldesenbet et al. (2017), which showed

488   the shifting of the river discharge more to overland flow mechanism in the last four to five decades

489   in the upper Blue Nile basin. However, the rate of hydrological change found in this study is

490   relatively small compared to the rate of land use change. This reinforces the idea that the land use

491   is not the primary important controlling factor compared to rainfall amount (discussed above in

492   detail). Similarly, Birhanu et al. (2019) found a negligible change of the water balance components

493   for Gumara catchment for the land use change of 1986-2015 using HBV model. Gashaw et al.

494   (2018) had also evaluated the effect of changing land use on the hydrology of Andassa catchment

495   (neighboring small catchment, south of Lake Tana basin) over the same period (1986-2015) using

496 SWAT model. Compared to this study, they found a similar amount of reduction in baseflow

497 (supposed to be equivalent to groundwater recharge), but a bit more runoff increment.

498 *Table 3. Long-term mean seasonal and annual groundwater recharge, runoff, and evapotranspiration values*

499 *simulated for land use of the years 1986, 2000, and 2014 using the WetSpass water balance model.*

Year	season	recharge (mm)	runoff (mm)	total evapotranspiration (mm)
1986	summer	247	379	424
	winter	81	33	337
	annual	**328**	**412**	**761**
2000	summer	243	381	427
	winter	79	33	338
	annual	**322**	**414**	**765**
2014	Summer	237	383	428
	winter	78	33	342
	annual	**315**	**416**	**770**

500 ## 4.4. Groundwater recharge estimation using WTF and CMB methods

501 The aquifer type, location, and hydrograph response for recharging periods for the 65 wells

502 are checked, and found as they are more or less fulfill the assumptions of the WTF method for

503 recharge estimation discussed in detail by Healy and Cook (2002). The seasonal recharge values

504 calculated for 2017, 2018, and some for 2019, are averaged out. Many rises and declines within

505 the overall recharging season are not considered. Only the seasonal highest rise and extrapolated

506 antecedent decline during the highest rise (using the graphical technique) has taken into account.

507 As a result, the calculated recharge is the total recharge that joined the groundwater.

508 The specific yield was estimated both using a literature compilation of Johnson (1967), and

509 through an empirical formula developed by Beretta and Stevenazzi (2018) for the wells where

510 pumping tests had been executed. The resulting specific yield values are highly variable depending

511 on primarily geology and degree of weathering. Hydrogeologically, the shallow monitoring wells

512 are placed on four hydrogeological units: weathered basaltic regolith, pyroclastic rocks, fractured

513 Quaternary basalt (with intermediate weathering grade), and alluvio-lacustrine formations. The

514 Quaternary basalt was found with the highest Sy value (ranging from 0.08 to 0.1), while for the

515   pyroclastic and alluvio-lacustrine deposits, values as low as 0.02 and as high as 0.074 were found.

516   The weathered basaltic regolith has a specific yield ranging from 0.04 to 0.08.

517
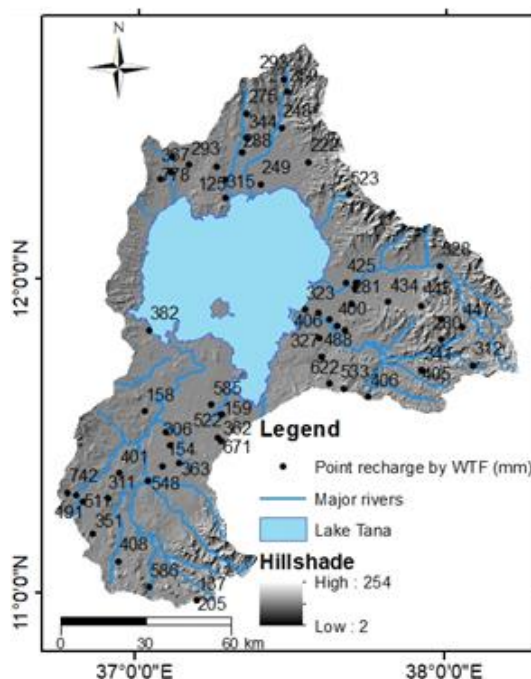
518   *Fig. 10. Point values of annual groundwater recharge estimated at 65 groundwater level monitoring wells.*

519   *The wells include shallow hand-dug wells, piezometers, and a few boreholes being monitored both*

520   *manually and using automatic pressure transducer device.*

521   The mean annual groundwater recharge using the WTF ranges from 125 mm to 778 mm,

522   accounting for about 9% to 54% of the mean basin rainfall. In general, the southern and eastern

523   (Gumara river catchment) part of the Lake Tana basin has higher recharge than the northern part

524   (Fig. 10). This is also similar to the result of the WetSpass model (Fig. 7a). It has an overall basin

525   average of 369 mm (26% of the rainfall), which is a bit higher than the mean average estimated by

526   the WetSpass model (22%). This could be due to the ability of the WTF method to catch up the

527   focused recharge through rock fractures, and/or lateral groundwater flow besides the diffuse

528   recharge from the direct precipitation that Yenehun et al. (2020) had thoroughly discussed. The

529   spatial variation of recharge depends on topography and geology. In steep sloping topography

530   aquifers, where low recharge is expected, higher recharge values by WTF compared to WetSpass

531   is estimated (Figs. 5c and 10). This is due to the additional recharge from the upstream area by

532 lateral groundwater flow in addition to the diffuse recharge from the direct rainfall Furthermore,

533 on the flat floodplain areas, the recharge estimated by the WTF is small. This is due to the

534 limitation of the aquifer storage. It means the aquifer is more or less fully recharged in the early to

535 middle of the recharge period (usually end of July to mid-August) but the model keeps on adding

536 the recharge as there is unlimited aquifer storage. In general, the WetSpass method is less effective

537 in the fractured aquifers where focused recharge is the important recharging mechanism and on

538 flat floodplain areas, which disregards both the storage limitation in the flat floodplain alluvial and

539 additional focused recharge in the fractured rock aquifers. In addition, it performs less in steeply

540 sloping aquifers where fast groundwater flow accumulates additional recharge through lateral

541 groundwater flow.

542   Similar to WetSpass and WTF methods, the recharge calculation using the CMB method

543 shows strong spatial variability. The groundwater recharge in the southern and eastern catchments

544 is higher than in the northern, and western catchments (Table 4). The mean annual recharge by the

545 CMB method is about 346 mm (24% of the rainfall). The spatial distribution is more or less similar

546 to the spatial distribution map simulated by WetSpass (Fig. 7a), and the point recharge distribution

547 of the WTF method (Fig. 10).

548 *Table 4. Estimated mean annual groundwater recharge amount using the CMB method for the different catchments*

549 *grouped based on similar runoff characteristics.*

Catchments	Number of analyzed GW points	Groundwater recharge (mm)
Southern	51	404
Eastern	65	355
Northern	15	164
Western	7	206

4.5. Summarizing groundwater recharge estimations by the different methods and comparing with other similar studies

552 The mean annual groundwater recharge values found with the three methods are 315 mm for

553 WetSpass, 369 mm for WTF, and 345 mm for CMB. The WetSpass value ranges from 0 mm to

554 1085 mm, WTF ranges from 125 mm to 778 mm, and CMB from 164 mm to 404 mm. The

555 relatively smaller range for CMB is due to the consideration of average values in the four

556 distinguished zones rather than at 138 groundwater sampling points. Otherwise, the range of values

557 would have been higher, given the wider range of chloride values (0.3 to 12.5 mg/l) of the

558 groundwater samples. The heterogeneity in recharge processes and recharge rates over the basin

559 is well notified by the higher range of values by the WetSpass and WTF methods.

560 Generally, recharge in the eastern and southern catchments is higher than in the northern

561 catchments (Table 5), primarily due to higher rainfall and favorable geology (highly fractured

562 Quaternary basalt) (Fig. 2). The recharge by CMB in the northern, and somewhat in the western

563 part is much smaller compared to the values by the other two methods (Table 5). This could be

564 due to some recharge from the river water which elevates the chloride concentration of the

565 groundwater which hence decreases the recharge value according to Eq. 5. The chloride

566 concentration in the river water is higher due to exposure to open water evaporation before

567 infiltration and percolation to the groundwater zone.

568 *Table 5. mean annual groundwater recharge values estimated for the different catchments by all CMB, WetSpass*

569 *and WTF methods.*

Catchments	Groundwater recharge by CMB (mm)	Groundwater recharge by WetSpass (mm)	Groundwater recharge by WTF (mm)
Southern	404	453	439
Eastern	355	372	435
Northern	164	315	303
Western	206	357	445

570 There are other recharge studies performed on different sub-catchments of the Lake Tana

571 basin. Abiy et al. (2016) applied a SWAT model for Rib and Gumara catchments and estimated

572 recharge to be 451 mm and 414 m, respectively (Table 5). In the WetSpass model of this study,

573 352 mm for Rib, and 392 mm for Gumara are estimated, a bit smaller than the study by Abiy et al.

574 (2016). Yenehun et al. (2020) applied four different techniques to estimate recharge on the upper

575 part of Gilgel Abay catchment, and hence, 431 mm, 477 mm, and 462 mm, were estimated as mean

576 annual values using SMB (soil moisture balance), CMB, and WetSpass. In the WetSpass model of

577 this study, 453 mm is the recharge amount for the whole Gilgel Abay catchment (Table 5), which

578 is very close to the result by Yenehun et al. (2020). Similarly, Yenehun et al. (2020) applied the

579 WTF method and estimated annual value ranging from 157 mm to 760 mm. Walker et al. (2019)

580   calculated the natural groundwater recharge using nine different methods in the Dangila area

581   (upper part of Gilgel Abay catchment). They estimated the mean annual recharge amount in the

582   range of 280-430 mm. Nigate et al. (2020) applied the WTF, CMB and SMB methods on Infranz

583   catchment, which is a small river catchment in the southern part of Lake Tana basin (Fig. 1). They

584   estimated 436 mm by CMB, values ranging from 400 and 800 mm by WTF, and 748 mm by SMB

585   as annual mean values. The results by these studies are more or less similar to the values found in

586   this study for those specific study areas. In the Infranz catchment, groundwater recharge is higher

587   than average, due to the focused recharge by fractured Quaternary basalt besides the direct

588   recharge. On the other hand, Mamo (2015) applied the CMB method for the whole Tana basin,

589   and estimated recharge to be 284 mm, which is underestimated compared to our results. This could

590   be due to using deep well groundwater chloride data which are more mineralized or due to rainfall

591   sampling period i.e. chloride concentration of rainfall is highly variable depending season

592   Different authors presented recharge values for different parts of Ethiopian aquifers. Ferede

593   et al. (2020) have applied WTF and CMB techniques at a small catchment on a rift valley volcanic

594   aquifer. They estimated recharge at 35% and 20% of rainfall, respectively by WTF and CMB,

595   while it is 26% for the former and 24% for the latter in our study. These results are comparabl.e

596   The relatively higher recharge by WTF in this rift valley volcanic aquifer could be due to the more

597   open fractures in Quaternary basalt that have significant focused recharge. The geology of rift

598   valley is Quaternary volcanic rocks where open fissures and fractures are very common (Paola,

599   1972). Tilahun et al. (2009) applied the WetSpass model on an area predominantly containing

600   sedimentary and basement rock aquifers in eastern Ethiopia. They estimated the mean annual

601   recharge value at 5% of rainfall. Similarly, Gebreyohannes et al. (2013) applied the same method

602   on sedimentary rock aquifers in northern Ethiopia, and found 6% of rainfall amount. Both

603   estimates are too small compared to this study. This could be due to the high-intensity nature of

604   the rainfall (especially for the former) as well as the focused recharge through faults, bedding

605   surfaces, and joints, which is characteristic of the geology of these areas and which water balance

606   models like WetSpass fail to capture. Demlie et al. (2007a) applied the CMB method, and found

607   23% of rainfall as a recharge value in a similar volcanic aquifer in central Ethiopia, which is close

608   to our result (24% of rainfall). Using unsaturated zone chloride measurement, supported by stable

609   isotopes, they quantified a significant amount of focused recharge at areas where faults and joints

610   dominate. These all assert our finding that water balance methods are less effective in estimating

611   recharge over areas where recharge by preferential flow is common.

5.   Conclusion

613   The physically-based water balance model, WetSpass has effectively been applied to simulate

614   the water balance components of Lake Tana basin, containing the largest lake of Ethiopia. The

615   model simulates the mean annual major river inflows with a coefficient of determination (R^2) of

616   80%. The model better simulated flows for the Gumara and Gilgel Abay river catchments than for

617   the other catchments where deep percolation might conceal the base flow from measurement by

618   the gauging stations. On the other hand, the WetSpass model applied is a quasi-steady state that

619   used long-term average seasonal rainfall amounts, though the rainfall characteristics vary within

620   fine time scales. This might limit the effectiveness of the model in simulating runoff amounts. The

621   annual groundwater recharge using WetSpass ranges from 0% of rainfall, at the water bodies where

622   infiltration is impossible, to 57% in the flat, silty loam, and bushland cover type. It has a mean

623   annual value of 315 mm (22% of the precipitation amount), of which 237 mm is recharged in

624   summer and the other 78 mm in the winter season. Similarly, the WTF and CMB methods have

625   also shown strong spatial variability, with higher recharge values in the southern and eastern

626   catchments, and lower in the northern and partly in the western parts, primarily due to rainfall

627   distribution and geology. There is good correlation between point recharge values by the WTF

628   and extracted recharge from the WetSpass spatial maps. However, there is a high disparity on

629   wells located on the storage-controlled flat floodplains and focused recharge affected fractured

630   rock aquifers. Hence, though water balance models estimate recharge at fine spatial scales that

631   help for water management in specific areas, its capacity is limited for aquifers where only diffuse

632   recharge is the main recharging mechanism and for those aquifers that are not fully saturated early

633   in the recharge period.

634   The mean annual runoff for the whole basin is about 416 mm (29% of the average

635   precipitation)and evapotranspiration is about 770 mm, which is 53% of the mean basin

636   precipitation. The precipitation amount is highly controlling the spatial distribution of the runoff,

637   more than the land use and soil. The mean evaporation over the lake is about 1485 mm. The spatial

638   distribution of the evapotranspiration over the basin is highly controlled by the rainfall and the

639 land cover types. The hydrology of the basin has not much changed in the last three decades though
640 cultivated land has expanded significantly.

Author Contribution

642 **Alemu Yenehun:** conceptualization, investigation, formal analysis, and writing - original draft

643 **Mekete Desssie:** project administration, conceptualization and investigation, writing- review and
644 editing

645 **Fenta Nigatie:** conceptualization and investigation, writing- review and editing

646 **Ashebir Sewale Belay:** conceptualization and investigation

647 **Mulugeta Azeze:** conceptualization, writing- review and editing

648 **Marc Van Camp:** conceptualization, formal analysis and Software

649 **Derbew Fenetie Taye:** data collection

650 **Desale Kidane:** writing- review and editing

651 **Enyew Adgo:** project administration, funding acquisition, writing- review and editing

652 **Jan Nyssen:** project administration, funding acquisition, writing- review and editing

653 **Ann van Griensven:** conceptualization, investigation

654 **Kristine Walraevens:** conceptualization, writing- review and editing, project administration and
655 supervision, validation.

Competing interests

657 The authors declare that they have no known competing financial interests or personal
658 relationships that could have appeared to influence the work reported in this paper.

Acknowledgment

660 This research work is funded by the Belgian Development Cooperation (VLIR-UOS)
661 through the BDU-IUC project. Hence, we would like to thank you VLIR-UOS for the funding,
662 and the project staff for facilitating our fieldwork activities. Furthermore, we want to extend our

663   thanks to our monitoring well data recorders, who had been consistently recording the data. We

664   would like also to extend our thanks to the Ethiopian Meteorological Agency, Bahir Dar Branch,

665   and different zonal and woreda water offices that help during monitoring well installation and data

666   recording personnel recruitment.

References

668   Abate, M., Nyssen, J., Moges, M.M., Enku, T., Zimale, F.A., Tilahun, S.A., Steenhuis, T.S., 2017. Long-
669   Term Landscape Changes in the Lake Tana Basin as Evidenced by Delta Development and
670   Floodplain Aggradation in Ethiopia. L. Degrad. Dev. 28, 1820–1830.

671   Abiy, A.Z., Demissie, S.S., Charlotte, M., Dessu, S.B., Melesse, A.M., 2016. Groundwater Recharge and
672   Contribution to the Tana Sub-basin, Upper Blue Nile Basin, Ethiopia, in: Landscape Dynamics,
673   Soils and Hydrological Processes in Varied Climates. pp. 463–481. https://doi.org/10.1007/978-3-
674   319-18787-7

675   ADSWE, 2015a. Tana sub basin integrated Land Use Planning and Environmental impact Study,
676   Technical Report: Land Use Land Cover and Change Detection.

677   ADSWE, 2015b. Tana sub basin Land Use Planning and Environmental Study Project, Technical Report
678   I: Soil Survey.

679   Alemayehu, T., Kebede, S., 2011. The role of geodiversity on the groundwater resource potential in the
680   upper Blue Nile River Basin, Ethiopia. Environ. Earth Sci. 64, 1283–1291.
681   https://doi.org/10.1007/s12665-011-0946-7

682   Allen, R.G., Pereira, L.S., Raes, D., Smith, M., 1998. Crop evapotranspiration-Guidelines for computing
683   crop water requirements-FAO Irrigation and drainage paper 56, FAO, Rome.

684   Allison, G.B., 1988. A Review of Some of the Physical, Chemical and Isotopic Techniques Available for
685   Estimating Groundwater Recharge, in: Springer. pp. 49–72.

686   Allison, M.., Hughes, G.., 1978. The use of environmental chloride and tritium to estimate total recharge
687   to an unconfined aquifer. Aust. J. Soil Res. 16, 181–195. https://doi.org/10.1071/SR9780181

688   Ashaolu, E.D., 2020. Spatial and temporal recharge estimation of the basement complex in Nigeria , West
689   Africa. J. Hydrol. Reg. Stud. 27, 100658. https://doi.org/10.1016/j.ejrh.2019.100658

690   Ayenew, T., Demlie, M., Wohnlich, S., 2008. Hydrogeological framework and occurrence of
691   groundwater in the Ethiopian aquifers. J. African Earth Sci. 52, 97–113.

692   https://doi.org/10.1016/j.jafrearsci.2008.06.006

693   Bakundukize, C., van Camp, M., Walraevens, K., 2011. Estimation of Groundwater Recharge in

694   Bugesera Region (Burundi) using Soil Moisture Budget Approach. Geol. Belgica 14, 85–102.

695   Batelaan, O., De Smedt, F., 2007. GIS-based recharge estimation by coupling surface-subsurface water

696   balances. J. Hydrol. 337, 337–355. https://doi.org/10.1016/j.jhydrol.2007.02.001

697   Batelaan, O., De Smedt, F., 2001. WetSpass: a flexible, GIS based, distributed recharge methodology for

698   regional groundwater modelling, in: Impact of Human Activity on Groundwater Dynamics. IAHS

699   Publ, pp. 11–18.

700   Beretta, G.P., Stevenazzi, S., 2018. Specific yield of aquifer evaluation by means of a new experimental

701   algorithm and its applications. Ital. J. Groundw. 24, 39–46. https://doi.org/10.7343/as-2018-325

702   Birhanu, A., Masih, I., van der Zaag, P., Nyssen, J., Cai, X., 2019. Impacts of land use and land cover

703   changes on hydrology of the Gumara catchment, Ethiopia. Phys. Chem. Earth 112, 165–174.

704   https://doi.org/10.1016/j.pce.2019.01.006

705   Chebud, Y.A., Melesse, A.M., 2009. Modelling lake stage and water balance of Lake Tana, Ethiopia.

706   Hydrol. Process. 23, 3534–3544. https://doi.org/10.1002/hyp.7416

707   Chorowicz, J., Collet, B., Bonavia, F.F., Mohr, P., Parrot, J.F., Korme, T., 1998. The Tana basin,

708   Ethiopia: Intra-plateau uplift, rifting and subsidence. Tectonophysics 295, 351–367.

709   https://doi.org/10.1016/S0040-1951(98)00128-0

710   Crosbie, R.S., Binning, P., Kalma, J.D., 2005. A time series approach to inferring groundwater recharge

711   using the water table fluctuation method. Water Resour. Res. 41, 1–9.

712   https://doi.org/10.1029/2004WR003077

713   Delin, G.N., Healy, R.W., Lorenz, D.L., Nimmo, J.R., 2007. Comparison of local- to regional-scale

714   estimates of ground-water recharge in Minnesota , USA. J. Hydrol. 334, 231–249.

715   https://doi.org/10.1016/j.jhydrol.2006.10.010

716   Demlie, M., Wohnlich, S., Ayenew, T., 2008. Major ion hydrochemistry and environmental isotope

717   signatures as a tool in assessing groundwater occurrence and its dynamics in a fractured volcanic

718   aquifer system located within a heavily urbanized catchment, central Ethiopia. J. Hydrol. 353, 175–

719   188. https://doi.org/10.1016/j.jhydrol.2008.02.009

720   Demlie, M., Wohnlich, S., Gizaw, B., Stichler, W., 2007a. Groundwater recharge in the Akaki catchment

721 , central Ethiopia : evidence from environmental isotopes (d 18 O , d 2 H and 3 H) and chloride

722 mass balance. Hydrol. Process. 21, 807–818. https://doi.org/10.1002/hyp.6273

723 Demlie, M., Wohnlich, S., Wisotzky, F., Gizaw, B., 2007b. Groundwater recharge, flow and

724 hydrogeochemical evolution in a complex volcanic aquifer system, central Ethiopia. Hydrogeol. J.

725 15, 1169–1181. https://doi.org/10.1007/s10040-007-0163-3

726 Dessie, M., Verhoest, N.E.C., Pauwels, V.R.N., Adgo, E., Deckers, J., Poesen, J., Nyssen, J., 2015. Water

727 balance of a lake with floodplain buffering: Lake Tana, Blue Nile Basin, Ethiopia. J. Hydrol. 522,

728 174–186. https://doi.org/10.1016/j.jhydrol.2014.12.049

729 Dessie, M., Verhoest, N.E.C., Pauwels, V.R.N., Admasu, T., Poesen, J., Adgo, E., Deckers, J., Nyssen, J.,

730 2014. Analyzing runoff processes through conceptual hydrological modeling in the Upper Blue Nile

731 Basin , Ethiopia 5149–5167. https://doi.org/10.5194/hess-18-5149-2014

732 Dile, Y.T., Tekleab, S., Kaba, E.A., Gebrehiwot, S.G., Worqlul, A.W., Bayabil, H.K., Yimam, Y.T.,

733 Tilahun, S.A., Daggupati, P., Karlberg, L., Srinivasan, R., 2018. Advances in water resources

734 research in the Upper Blue Nile basin and the way forward: A review. J. Hydrol. 560, 407–423.

735 https://doi.org/10.1016/j.jhydrol.2018.03.042

736 Enku, T., Tadesse, A., Yilak, D.L., Gessesse, A.A., Addisie, M.B., Abate, M., Zimale, F.A., Moges,

737 M.A., Tilahun, S.A., Steenhuis, T.S., 2014. Biohydrology of low flows in the humid Ethiopian

738 highlands: The Gilgel Abay catchment. Biol. 69, 1502–1509. https://doi.org/10.2478/s11756-014-

739 0462-9

740 Ferede, M., Haile, A.T., Walker, D., Gowing, J., 2020. Multi-method groundwater recharge estimation at

741 Eshito micro-watershed , Rift Valley Basin in Ethiopia. Hydrol. Sci. J. 65, 1596–1605.

742 https://doi.org/10.1080/02626667.2020.1762887

743 Gashaw, T., Tulu, T., Argaw, M., Worqlul, A.W., 2018. Modeling the hydrological impacts of land

744 use/land cover changes in the Andassa watershed, Blue Nile Basin, Ethiopia. Sci. Total Environ.

745 619–620, 1394–1408. https://doi.org/10.1016/j.scitotenv.2017.11.191

746 Gebremicael, T.G., Mohamed, Y.A., Betrie, G.D., van der Zaag, P., Teferi, E., 2013. Trend analysis of

747 runoff and sediment fluxes in the Upper Blue Nile basin: A combined analysis of statistical tests,

748 physically-based models and landuse maps. J. Hydrol. 482, 57–68.

749 https://doi.org/10.1016/j.jhydrol.2012.12.023

750 Gebreyohannes, T., De Smedt, F., Walraevens, K., Gebresilassie, S., Hussien, A., Hagos, M., Amare, K.,

751   Deckers, J., Gebrehiwot, K., 2013. Application of a spatially distributed water balance model for
752   assessing surface water and groundwater resources in the Geba basin, Tigray, Ethiopia. J. Hydrol.
753   499, 110–123. https://doi.org/http://dx.doi.org/10.1016/j.jhydrol.2013.06.026

754   Graf, R., Przybyłek, J., 2018. Application of the WetSpass simulation model for determining conditions
755   governing the recharge of shallow groundwater in the Poznań Upland, Poland. Geologos 24, 189–
756   205. https://doi.org/10.2478/logos-2018-0020

757   Guan, H., Love, A.J., Simmons, C.T., Hutson, J., Ding, Z., 2010. Catchment conceptualisation for
758   examining applicability of chloride mass balance method in an area with historical forest clearance.
759   Hydrol. Earth Syst. Sci. 14, 1233–1245. https://doi.org/10.5194/hess-14-1233-2010

760   Healy, R.W., Cook, P.G., 2002. Using groundwater levels to estimate recharge. Hydrogeol. J. 10, 91–109.

761   Hornero, J., Manzano, M., Ortega, L., Custodio, E., 2016. Environment Integrating soil water and tracer
762   balances , numerical modelling and GIS tools to estimate regional groundwater recharge :
763   Application to the Alcadozo Aquifer System (SE Spain). Sci. Total Environ. 568, 415–432.
764   https://doi.org/10.1016/j.scitotenv.2016.06.011

765   Hurni, H., Tato, K., Zeleke, G., 2005. The Implications of Changes in Population, Land Use, and Land
766   Management for Surface Runoff in the Upper Nile Basin Area of Ethiopia. Mt. Res. Dev. 25, 147–
767   154. https://doi.org/10.1659/0276-4741(2005)025[0147:TIOCIP]2.0.CO;2

768   Jepsen, D.H., Athearn, M.J., 1961. A general Geologic map of the Blue Nile River Basin, Ethiopia (1: 1,
769   000, 000), Department of Water Resources, Addis Ababa.

770   Johnson, A.I., 1967. Specific yield: compilation of specific yields for various materials. US Gov. Print.
771   Off.

772   Kebede, S., Travi, Y., Alemayehu, T., Ayenew, T., 2005. Groundwater recharge, circulation and
773   geochemical evolution in the source region of the Blue Nile River, Ethiopia. Appl. Geochemistry
774   20, 1658–1676. https://doi.org/10.1016/j.apgeochem.2005.04.016

775   Kebede, S., Travi, Y., Alemayehu, T., Marc, V., 2006. Water balance of Lake Tana and its sensitivity to
776   fluctuations in rainfall, Blue Nile basin, Ethiopia. J. Hydrol. 316, 233–247.
777   https://doi.org/10.1016/j.jhydrol.2005.05.011

778   Mamo, S., 2015. Integrated Hydrological and Hydrogeological System Analysis of the Lake Tana Basin,
779   Northwestern Ethiopia. PhD Thesis, Addis Ababa, Ethiopia.

780   Manna, F., Cherry, J.A., Mcwhorter, D.B., Parker, B.L., 2016. Groundwater recharge assessment in an
781   upland sandstone aquifer of southern California. J. Hydrol. 541, 787–799.
782   https://doi.org/10.1016/j.jhydrol.2016.07.039

783   Marechal, J.C., Dewandel, B., Ahmed, S., Galeazzi, L., Zaidi, F.K., 2006. Combined estimation of
784   specific yield and natural recharge in a semi-arid groundwater basin with irrigated agriculture. J.
785   Hydrol. 329, 281–293. https://doi.org/10.1016/j.jhydrol.2006.02.022

786   Minucci, E., 1938. Ricerche geologiche nella regione del Tana. Missione di Studio al Lago Tana. R.
787   Accad. Ital 1, 19–36.

788   Moon, S.K., Woo, N.C., Lee, K.S., 2004. Statistical analysis of hydrographs and water-table fluctuation
789   to estimate groundwater recharge. J. Hydrol. 292, 198–209.
790   https://doi.org/10.1016/j.jhydrol.2003.12.030

791   Nigate, F., 2019. Investigating the hydrogeological system of the Lake Tana basin in the northwestern
792   highlands of Ethiopia (the Upper Blue Nile). Gelogy Department, Ghent University, Belgium.

793   Nigate, F., Camp, M. Van, Yenehun, A., Belay, A.S., Walravaens, K., 2020. Recharge – Discharge
794   Relations of Groundwater in Volcanic Terrain of Semi-Humid Tropical Highlands of Ethiopia : The
795   Case of Infranz Springs , in the Upper. Water 12, 1–18.

796   Obuobie, E., Diekkrueger, B., Agyekum, W., Agodzo, S., 2012. Groundwater level monitoring and
797   recharge estimation in the White Volta River basin of Ghana. J. African Earth Sci. 71–72, 80–86.
798   https://doi.org/10.1016/j.jafrearsci.2012.06.005

799   Paola, G.M.D.I., 1972. The Ethiopian Rift Valley (Between 7 ° Off and 8 ° 40 ’ lat . North). Bull.
800   Volcanol. 36, 517–560.

801   Rientjes, T.H.M., Perera, B.U.J., Haile, A.T., Reggiani, P., Muthuwatta, L.P., 2011. Regionalisation for
802   lake level simulation - The case of Lake Tana in the Upper Blue Nile, Ethiopia. Hydrol. Earth Syst.
803   Sci. 15, 1167–1183. https://doi.org/10.5194/hess-15-1167-2011

804   Scanlon, B.R., Healy, R.W., Cook, P.G., 2002. Choosing appropriate techniques for quantifying
805   groundwater recharge. Hydrogeol. J. 10, 18–39.

806   Setegn, S., Srinivasan, R., Dargahi, B., 2008. Hydrological Modelling in the Lake Tana Basin, Ethiopia
807   Using SWAT Model. Open Hydrol. J. 2, 49–62.

808   SMEC, 2008. Hydrological Study of the Tana-Beles Sub-basins: Surface Water Investigations. Addis

809   Ababa, Ethiopia.

810   Somaratne, N., Smettem, K.R.J., 2014. Theory of the generalized chloride mass balance method for
811   recharge estimation in groundwater basins characterised by point and diffuse recharge. Hydrol.
812   Earth Syst. Sci. Discuss. 11, 307–332. https://doi.org/10.5194/hessd-11-307-2014

813   Tekleab, S., Uhlenbrook, S., Mohamed, Y., Savenije, H.H.G., Temesgen, M., Wenninger, J., 2011. Water
814   balance modeling of Upper Blue Nile catchments using a top-down approach. Hydrol. Earth Syst.
815   Sci. 15, 2179–2193. https://doi.org/10.5194/hess-15-2179-2011

816   Tesemma, Z.K., Mohamed, Y.A., Steenhuis, T.S., 2010. Trends in rainfall and runoff in the Blue Nile
817   Basin : 1964 – 2003. Hydrol. Process. 24, 3747–3758. https://doi.org/10.1002/hyp.7893

818   Tilahun, K., Merkel, B.J., 2009. Estimation of groundwater recharge using a GIS-based distributed water
819   balance model in Dire Dawa, Ethiopia. Hydrogeol. J. 17, 1443–1457.
820   https://doi.org/10.1007/s10040-009-0455-x

821   Uugulu, S., Wanke, H., 2020. Estimation of groundwater recharge in savannah aquifers along a
822   precipitation gradient using chloride mass balance method and environmental isotopes, Namibia.
823   Phys. Chem. Earth 116, 102844. https://doi.org/10.1016/j.pce.2020.102844

824   Wale, A., Rientjes, T.H.M., Gieske, A.S.M., Getachew, H.A., 2009. Ungauged catchment contributions to
825   Lake Tana ' s water 3693, 3682–3693. https://doi.org/10.1002/hyp

826   Walker, D., Parkin, G., Schmitter, P., Gowing, J., Tilahun, S.A., Haile, A.T., Yimam, A.Y., 2019.
827   Insights From a Multi-Method Recharge Estimation Comparison Study. Groundwater 57, 245–258.
828   https://doi.org/10.1111/gwat.12801

829   Woldesenbet, T.A., Elagib, N.A., Ribbe, L., Heinrich, J., 2017. Hydrological responses to land use/cover
830   changes in the source region of the Upper Blue Nile Basin, Ethiopia. Sci. Total Environ. 575, 724–
831   741. https://doi.org/10.1016/j.scitotenv.2016.09.124

832   Yenehun, A., Nigate, F., Belay, A.S., Desta, M.T., Van Camp, M., Walraevens, K., 2020. Groundwater
833   recharge and water table response to changing conditions for aquifers at different physiography: The
834   case of a semi-humid river catchment, northwestern highlands of Ethiopia. Sci. Total Environ. 748,
835   142243. https://doi.org/10.1016/j.scitotenv.2020.142243

836   Zhu, R., Croke, B.F.W., Jakeman, A.J., 2020. Diffuse groundwater recharge estimation confronting
837   hydrological modelling uncertainty. J. Hydrol. 584, 124642.
838   https://doi.org/10.1016/j.jhydrol.2020.124642